



Nanomechanical Unfolding of Self-Folded Graphene on Flat Substrate

C.L. Yi¹ · L.Y. Zhang^{2,3} · X.M. Chen^{1,3} · X.Q. Wang² · C.H. Ke^{1,4}

Received: 15 May 2018 / Accepted: 18 December 2018 / Published online: 22 January 2019
© Society for Experimental Mechanics 2019

Abstract

We report the nanomechanical unfolding of individual self-folded graphene flakes on a flat substrate by using atomic force microscopy techniques. The nanomechanical measurements and molecular dynamics simulations reveal the detailed unfolding process that turns a z-shaped self-folded graphene segment into a flat membrane. A reversible sliding phenomenon in the adhered graphene region during the unfolding process is observed. The findings are useful to better understand the reversible folding properties of graphene and in pursuit of reversible and morphing graphene origami.

Keywords Graphene · Unfolding · Origami · Atomic force microscopy

Introduction

The reversible mechanical deformability of graphene is of great importance to its functional properties [1–3] and many of its applications (e.g., graphene *origami* and *kirigami* [4]). The folded graphene has been studied using a variety of experimental, theoretical, and computational techniques [5–16]. However, the reported studies on the unfolding behavior of folded graphene sheets [17, 18] in the literature remain limited. By means of an unfolding operation, self-folded graphene can either return back to its flat state or enter new folding states. Unfolding is also an essential process in the investigation of the reversible folding deformability of graphene. The reported graphene unfolding work in the literature focuses on

studying the unfolding of large-scale graphene films [16, 19], in which local graphene deformations in the unfolding process remain inaccessible. Here we investigate the nanomechanical unfolding of single self-folded graphene flakes on flat substrates by using atomic force microscopy (AFM) – based nanomechanical manipulation and molecular dynamics (MD) simulations techniques.

Results and Discussion

Nanomechanical Unfolding of Self-Folded Graphene by Atomic Force Microscopy

We present one representative unfolding experiment that was performed on a self-folded accordion-shape graphene sheet, as displayed in Fig. 1(a). The displayed graphene was manufactured by using a mechanically exfoliated flat triangular-shape graphene sheet from a highly ordered pyrolytic graphite (HOPG) film [20] in a two-step folding process inside an AFM. The triangular graphene sheet, which was measured to be about 3 nm in thickness and estimated to be a seven-layer graphene, was first folded into a z-shape conformation on a silicon substrate through a buckling delamination process [12]. In the second folding step, the top triangular segment was folded up during an AFM contact-mode scan, which was presumably ascribed to the graphene-AFM tip adhesion interaction. The final self-folded graphene sheet was composed of three folds with three folding edges and a small triangular segment staying on top.

Electronic supplementary material The online version of this article (<https://doi.org/10.1007/s11340-018-00466-z>) contains supplementary material, which is available to authorized users.

✉ X.Q. Wang
xqwang@uga.edu

✉ C.H. Ke
cke@binghamton.edu

- ¹ Department of Mechanical Engineering, State University of New York at Binghamton, Binghamton, NY 13902, USA
- ² College of Engineering, University of Georgia, Athens, GA 30602, USA
- ³ State Key Laboratory for Manufacturing Systems Engineering, Xi'an Jiaotong University, Xi'an 710049, Shaanxi, China
- ⁴ Materials Science and Engineering Program, State University of New York at Binghamton, Binghamton, NY 13902, USA



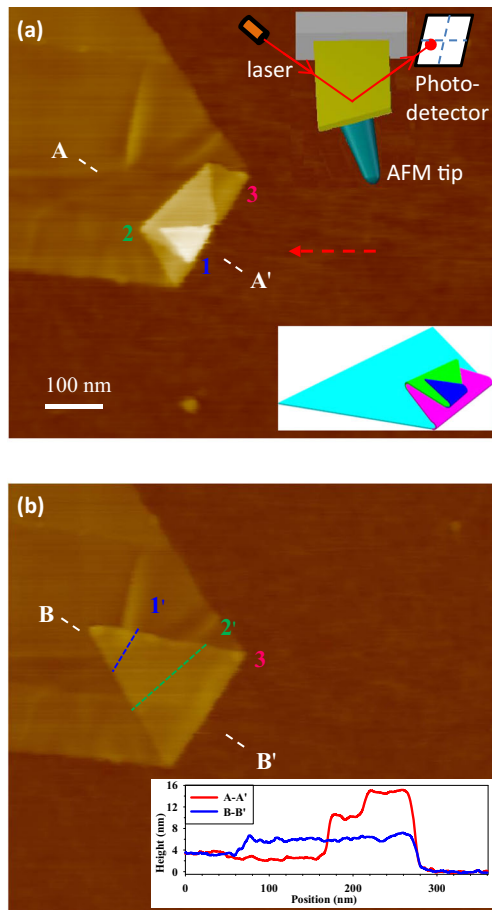


Fig. 1 AFM-based nanomechanical unfolding of a self-folded graphene on a flat substrate. **(a)** AFM topography image of a self-folded graphene. A 3D schematic drawing is inserted as a visualization aid. The top-right insert illustrates the unfolding approach using an AFM tip. The red dashed arrow indicates the moving direction of the AFM tip in the horizontal direction. **(b)** AFM topography image of the unfolded graphene. The inset plots show two AFM topography line profiles along the marked cross-section A-A' in **(a)** and B-B' before and after graphene unfolding. All scale bars represent 100 nm

The unfolding experiments were conducted inside a Park Systems XE-70 AFM using silicon AFM probes that have a measured tip radius of 10–20 nm and individually calibrated normal and torsional spring constants of 0.09–0.25 N/m and 0.039–0.11 nN/mV, respectively [21]. The self-folded graphene was unfolded by using an AFM tip that scanned laterally. The scan of the AFM tip was controlled to be unidirectional in both horizontal and vertical directions; namely from right to left and from bottom to top. The AFM scan rate was set at 500 nm/s and its vertical moving step was set to be 2 nm. The AFM unfolding scan started with a compressive load (i.e., set-point) of 0.05 nN, which was subsequently increased to 1, 5, 10 nN, respectively. AFM contact-mode imaging of the entire folded graphene region with a set point of 0.05 nN

was performed using the same AFM tip after each unfolding area-scan to confirm its present conformation. Graphene unfolding occurred during one of the unfolding area-scans with a compressive load of 10 nN, which was informed by the change in the recorded AFM topography line profiles. The subsequent AFM imaging shows that the original two-fold (z-shape) graphene segment was fully unfolded and stayed in a flat and fully extended conformation, which is displayed in Fig. 1(b). There was no sign of permanent deformation in the unfolded segment of the graphene (including the folding edges), which indicates an elastic deformation in graphene during its unfolding process. The AFM image also reveals that the unfolding occurred only for the upper two folds of the graphene, while the bottom fold remained intact. This is probably due to a larger adhering area and the resulting stronger adhesion interaction for the bottom fold compared with the other two folds. The blue and green dashed lines (i.e., 1' and 2') marked in Fig. 1(b) indicate the respective new positions of the two folding edges in the upper two folds (i.e., 1 and 2 as marked in Fig. 1(a)) in its unfolded conformation. The bottom insert in Fig. 1(b) shows two topography profiles of the self-folded graphene and its unfolded conformation along A-A' and B-B' cross-sections, respectively.

The AFM measurements show that the deformations of the folded graphene during the AFM unfolding scan (before the occurrence of unfolding) were reversible. Figure 2(a)–(d) show the AFM area-scan topography images of the selected folded graphene region under a compressive load of 0.05, 1, 5 and 10 nN, respectively. Figure 2(e) shows four selected AFM line-scanning topography and the corresponding lateral force profiles that were recorded at approximately the same scan location (as marked by the white dashed line C-C' in Fig. 2(a)) under each load. Graphene unfolding occurred along the scan path D-D' as marked in Fig. 2(d) under a compressive load of 10 nN. The corresponding topography and lateral force profiles are displayed in Fig. 2(e). The AFM images show that the position of the upper folding edge slid towards the left (along with the AFM scan direction), and the slide was more pronounced under a larger compressive load. It is noticed that the slide was rather uniform along the folding edge and measured to be about 5.3 nm for the 1 nN compressive load, about 17 nm for the 5 nN load, and about 27 nm for the 10 nN load. The measured slides coincide well with the positions of the peak lateral force observed from the recorded lateral force profiles. It is noticed from the AFM images in Fig. 2 that the upper triangular graphene segment underwent

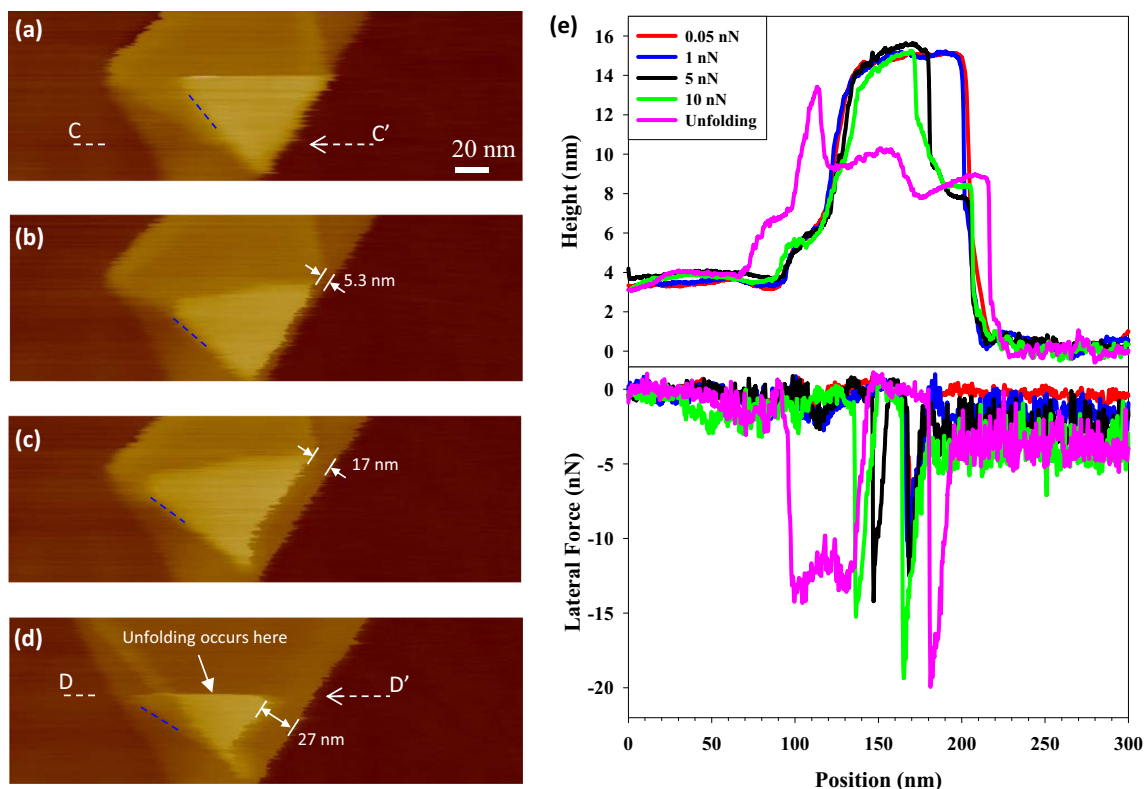


Fig. 2 (a)–(d) AFM topographic images recorded during the AFM unfolding area-scans with compressive loads of 0.05 nN, 1 nN, 5 nN and 10 nN, respectively (all scale bars 20 nm). Blue dashed lines along the graphene edge are added to aid visualisation of the rotation of the upper graphene segment. The orientation angles of the blue dashed line with respect to the horizontal direction are measured to be about 50° in (a), 41° in (b), 36° in (c), and 32° in (d). (e) Selected AFM height and the corresponding lateral force line profiles recorded at each compressive load along the marked position C–C' (before unfolding occurred) and also along the position D–D' where the graphene unfolding event occurred

not only translations, but also rotations, which is informed by the orientation change of its edge that is indicated by the blue dashed lines. It is concluded that the observed graphene folding edge slide was caused by the pushing of the AFM tip and is a clear indication of the interlayer sliding in the adhered graphene region. The displayed folding edge slides under compressive loads of 1 nN and 5 nN disappeared in the respective subsequent AFM topography images, indicating that the graphene deformation caused by the AFM tip was fully reversible. It is noted that the reversible unfolding of graphene has been observed in multiple measurements. Figure 3 shows selected AFM snapshots of another reversible folding and unfolding measurement. A flat triangular graphene segment of about 9.2 nm in thickness (Fig. 3(a)) was first partially folded by an AFM tip that was controlled to move along the red arrow path. Subsequently, the folded segment of about 5.0 nm in thickness (Fig. 3(b)) was unfolded back to its original flat conformation (Fig. 3(c)) by using the same AFM tip moving along the blue arrow path (Fig. 3(b)).

Molecular Dynamics Simulations of Graphene Unfolding Process

We perform MD simulations to better understand the conformation transitions of the self-folded graphene during its unfolding process, in particular to provide insights into atomistic details that are critical to graphene unfolding, and yet not accessible by experiments. MD simulations are performed based on the AIREBO potential [22]. In our simulations, one originally flat equilateral triangle-shaped monolayer graphene with an edge of 100 nm in length and an internal apex angle of 60° is first mechanically folded into a stable 3-fold structure, and is then placed on top of a flat silicon oxide substrate. The relaxed self-folded graphene on the substrate is displayed in Fig. 4(a), which is conformationally close to the graphene probed in the unfolding experiment as shown in Fig. 1. A cone-shaped AFM tip, which is composed of 15, 215 silicon atoms and has a height of 6.25 nm, is placed 1.5 nm above the substrate surface. The AFM tip moves at a speed of 0.05 nm/ps along the angle bisector direction of the triangle-shaped graphene sheet.

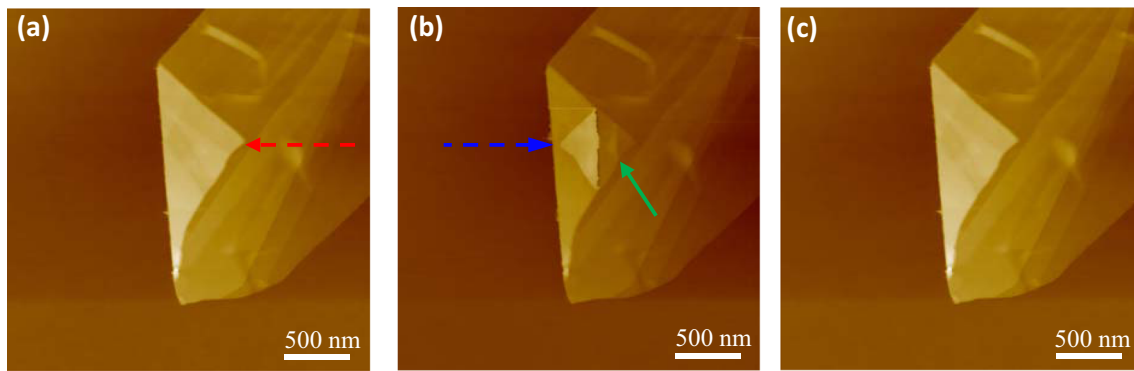
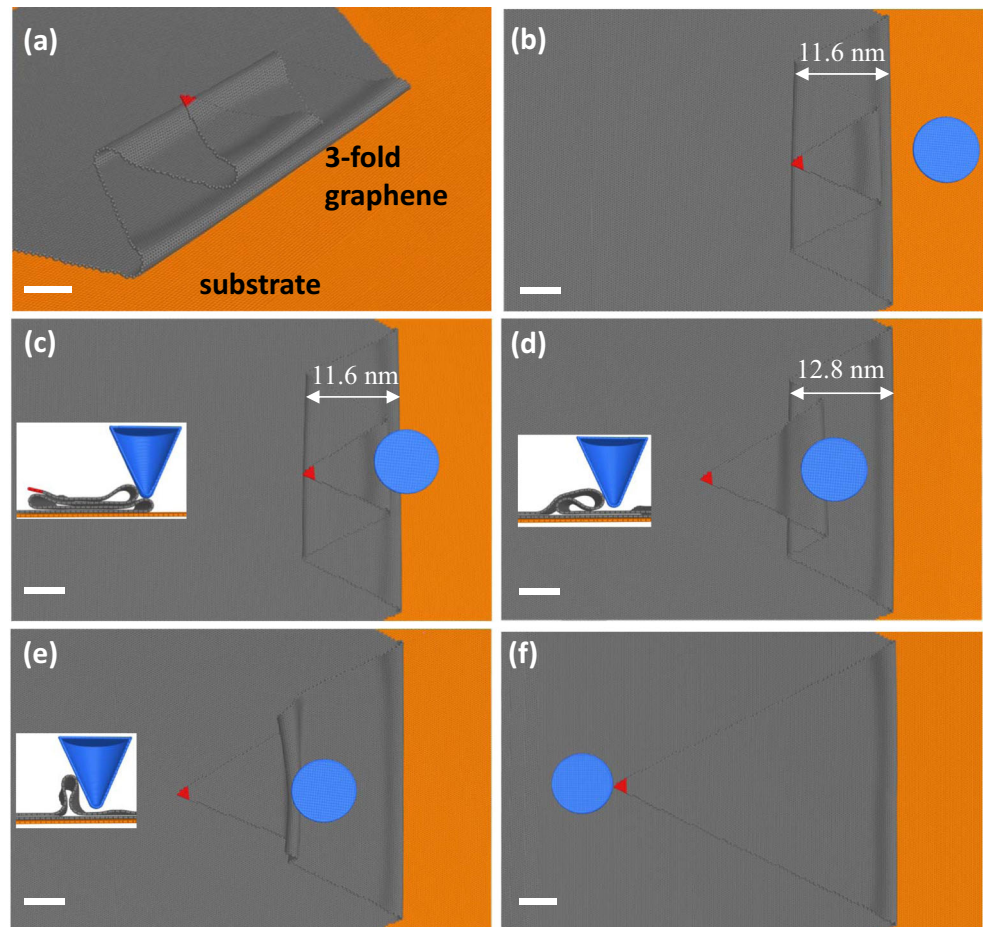


Fig. 3 Selected AFM snapshots of one graphene folding and unfolding measurement. **(a)** The original conformation of a triangular graphene segment (about 9.2 nm in thickness) as part of one folded graphene. **(b)** The partially folded graphene segment (about 5.0 nm in thickness). The green arrow indicates the intact portion of the graphene segment that was measured to be about 4.2 nm in thickness. **(c)** The unfolded graphene segment. The red and blue arrows indicate the respective moving paths of the AFM tip in the folding and unfolding processes

Figure 4(b)–(f) show five selected MD snapshots of the graphene unfolding process. MD simulations reveal that the continuous forward motion of the AFM tip successively breaks the bending stability of the upper two folds until the upper two graphene layers unfold completely flat onto the bottom graphene layer. In detail, with the upper folding edge of being pushed

forward by the AFM tip, the upper graphene layer slides forward, which is accompanied by a rolling of the bottom graphene layer in the upper fold (Fig. 4(d)). As a result, the graphene corner (shown in red in Fig. 4) climbs over and down the folding edge of the middle fold, and the top graphene layer slides onto the bottom graphene layer. The effective contact area

Fig. 4 Selected MD simulation snapshots displaying the unfolding of a self-folded mono-layer graphene that stays on a silicon substrate by using an AFM tip (all scale bars 5 nm). The insets show the corresponding cross-sectional view of the conformation of the graphene and its contact with the AFM tip. **(a)** 3D view and **(b)** top view of the initial self-folded graphene conformation; **(c)** initial contact between the graphene and the AFM tip; **(d)**, **(e)** two intermediate unfolding conformations; **(f)** the final unfolded conformation. The blue dot represents the AFM probe tip. The red triangle indicates the apex of the upper triangular graphene segment



between these two layers continuously increases until the upper and the middle folds merge into a single out-of-plane fold as shown in Fig. 4(e). The out-of-plane fold slowly vanishes as the top graphene layer continues to slide on the bottom graphene layer (Fig. 4(f)).

The MD simulations reveal that the initial forward-sliding of the upper graphene folding edge (up to 2.5 nm) caused by the AFM tip pushing at the beginning of the unfolding process is fully reversible, which is qualitatively consistent with our AFM experimental findings. Further AFM pushing results in the upper forefront graphene to make a larger area contact with the bottom graphene segment, and the resulting adhesion interaction prevents the graphene from returning back to its original conformation even if the AFM tip is removed from the system.

It is noted that the graphene unfolding process is influenced by a number of factors, such as the number of layers in graphene and its stacking interactions. Two stacked graphene sheets can stay in either AA or AB modes, which correspond to the incommensurate and commensurate stacking orders, respectively. The AB-stacked graphene is shown to be energetically more stable (see Fig. S1 in supplementary materials) and more likely occurs in the folded structure. The commensurate stacking order will inevitably introduce a twist to the folded graphene (see Fig. S2) and increase the resistance to the relative slide between the stacked graphene sheets [23–25]. We perform MD simulations to provide insights into the influence of the stacking mode on the graphene unfolding process. The results, which are shown in Fig. S3, reveal that the stacking mode has a substantial influence on the force needed to initiate the sliding in the stacked graphene, but the influence starts to fade rapidly as the slide continues and mostly vanishes as the stacked graphene starts to slide in alternative AB and AA modes. The MD results suggest that only the initial graphene unfolding stage is substantially affected by the graphene stacking mode.

Conclusion

In summary, we investigate the mechanical unfolding of self-folded graphene on flat substrates by using AFM manipulations and MD simulations. The study reveals a reversible sliding phenomenon between the adhered graphene layers that eventually turns a two-fold graphene segment into a flat membrane. The study demonstrates that it is feasible to mechanically manipulate and control the folding conformation of individual graphene in an active manner using AFM. The findings are useful in better understanding of the reversible folding properties of graphene and in pursuit of its reversible and morphing origami applications.

Acknowledgments C.L. Yi and L.Y. Z. contributed equally to this work. This work was supported by the National Science Foundation under Grant Nos. CMMI-1537333 (CK) and CMMI-1306065(XW). L.Y.Z. was supported by the National Natural Science Foundation of China (NSFC) under the Grant No. 31741043 and No. 51805414.

Publisher's Note Springer Nature remains neutral with regard to jurisdictional claims in published maps and institutional affiliations.

References

1. Al-Mulla T, Qin Z, Buehler MJ (2015) Crumpling deformation regimes of monolayer graphene on substrate: a molecular mechanics study. *J Phys Condens Matter* 27:345401. <https://doi.org/10.1088/0953-8984/27/34/345401>
2. Zhu W, Low T, Perebeinos V et al (2012) Structure and electronic transport in graphene wrinkles. *Nano Lett* 12:3431–3436. <https://doi.org/10.1021/nl300563h>
3. Kim K, Lee Z, Malone BD et al (2011) Multiply folded graphene. *Phys Rev B* 83:245433. <https://doi.org/10.1103/PhysRevB.83.245433>
4. Bles MK, Barnard AW, Rose PA et al (2015) Graphene kirigami. *Nature* 524:204–207. <https://doi.org/10.1038/nature14588>
5. Zhu S, Li T (2014) Hydrogenation-assisted graphene origami and its application in programmable molecular mass uptake, storage, and release. *ACS Nano* 8:2864–2872. <https://doi.org/10.1021/nn500025t>
6. Becton M, Zhang L, Wang X (2013) Effects of surface dopants on graphene folding by molecular simulations. *Chem Phys Lett* 584:135–141. <https://doi.org/10.1016/j.cplett.2013.08.027>
7. Zhang L, Zeng X, Wang X (2013) Programmable hydrogenation of graphene for novel nanocages. *Sci Rep* 3. <https://doi.org/10.1038/srep03162>
8. Meng X, Li M, Kang Z et al (2013) Mechanics of self-folding of single-layer graphene. *J Phys Appl Phys* 46:055308. <https://doi.org/10.1088/0022-3727/46/5/055308>
9. Cranford S, Sen D, Buehler MJ (2009) Meso-origami: folding multilayer graphene sheets. *Appl Phys Lett* 95:123121. <https://doi.org/10.1063/1.3223783>
10. Zhou Z, Qian D, Vasudevan VK, Ruoff RS (2012) Folding mechanics of bi-layer graphene sheet. *Nano LIFE* 02:1240007. <https://doi.org/10.1142/S1793984412400077>
11. Chen X, Yi C, Ke C (2015) Bending stiffness and interlayer shear modulus of few-layer graphene. *Appl Phys Lett* 106:101907. <https://doi.org/10.1063/1.4915075>
12. Yi C, Chen X, Zhang L et al (2016) Nanomechanical z-shape folding of graphene on flat substrate. *Extreme Mech Lett* 9:84–90. <https://doi.org/10.1016/j.eml.2016.05.008>
13. Chen X, Zhang L, Zhao Y et al (2014) Graphene folding on flat substrates. *J Appl Phys* 116:164301. <https://doi.org/10.1063/1.4898760>
14. Annett J, Cross GLW (2016) Self-assembly of graphene ribbons by spontaneous self-tearing and peeling from a substrate. *Nature* 535:271–275. <https://doi.org/10.1038/nature18304>
15. He Z-Z, Zhu Y-B, Wu H-A (2018) Self-folding mechanics of graphene tearing and peeling from a substrate. *Front Phys* 13:138111. <https://doi.org/10.1007/s11467-018-0755-5>
16. Zang J, Ryu S, Pugno N et al (2013) Multifunctionality and control of the crumpling and unfolding of large-area graphene. *Nat Mater* 12:321–325. <https://doi.org/10.1038/nmat3542>



17. Xu W, Qin Z, Chen C-T et al (2017) Ultrathin thermoresponsive self-folding 3D graphene. *Sci Adv* 3:e1701084. <https://doi.org/10.1126/sciadv.1701084>
18. Miskin MZ, Dorsey KJ, Bircan B et al (2018) Graphene-based bimorphs for micron-sized, autonomous origami machines. *Proc Natl Acad Sci*:201712889. <https://doi.org/10.1073/pnas.1712889115>
19. Parviz D, Metzler SD, Das S et al (2015) Tailored crumpling and unfolding of spray-dried pristine graphene and graphene oxide sheets. *Small* 11:2661–2668. <https://doi.org/10.1002/sml.201403466>
20. Novoselov KS, Geim AK, Morozov SV et al (2004) Electric field effect in atomically thin carbon films. *Science* 306:666–669. <https://doi.org/10.1126/science.1102896>
21. Qu W, Chen X, Ke C (2017) Temperature-dependent frictional properties of ultra-thin boron nitride nanosheets. *Appl Phys Lett* 110:143110. <https://doi.org/10.1063/1.4979835>
22. Stuart SJ, Tutein AB, Harrison JA (2000) A reactive potential for hydrocarbons with intermolecular interactions. *J Chem Phys* 112:6472–6486. <https://doi.org/10.1063/1.481208>
23. Koren E, Duerig U (2016) Moiré scaling of the sliding force in twisted bilayer graphene. *Phys Rev B* 94:045401. <https://doi.org/10.1103/PhysRevB.94.045401>
24. Koren E, Lörtscher E, Rawlings C et al (2015) Adhesion and friction in mesoscopic graphite contacts. *Science* 348:679–683. <https://doi.org/10.1126/science.aaa4157>
25. Zheng Q, Liu Z (2014) Experimental advances in superlubricity. *Friction* 2:182–192. <https://doi.org/10.1007/s40544-014-0056-0>